Investigating The Relationship between Land Surface Temperature (LST) and The Expansion of Built-up Land, A case Study of Baghdad, Iraq

Noor Waleed *, Maythm AL-Bakri

Department of Surveying, College of Engineering, University of Baghdad, Baghdad, Iraq

Abstract

   Converting green areas and agricultural land into built-up areas is one of the most significant effects of urbanization in Iraqi cities. Greenery spaces are a fundamental requirement for any city because they promote a healthy lifestyle and preserve urban areas' aesthetic and ecological beauty. The current study examines urbanization's effect on Baghdad city vegetation and land surface temperature. The Normalized Difference Built-Up Index (NDBI), Normalized Difference Vegetation Index (NDVI), Normalized Difference Water Index (NDWI), and Land Surface Temperature (LST) over Baghdad were used to determine the relationship among urban areas, vegetation areas, water bodies, and land temperature. The Baghdad-vector-data from the General Survey Authority was used along with Landsat Thematic Mapper for 2004 and 2008 and Landsat Operational Land Imager for 2013, 2017, and 2021. In order to understand the correlation between urban areas, water bodies, and green areas with LST, a correlation was carried out using ArcGIS software, and a scatter diagram was made to evaluate the relationship among the elements. The results showed that the temperature increased on Baghdad's land surface between 2004 and 2021. Moreover, built-up areas increased from 17% in 2004 to 53.2% in 2021; in contrast, the green areas drastically declined by 39.7%.

التحقيق في العلاقة بين درجة حرارة سطح الارض وتوسع الأراضي المبنية، محافظة بغداد، العراق حالة دراسة

نور وليد يونس *, ميثم مطشر البكري

[1]قسم المساحة, كلية الهندسة, جامعة بغداد, محافظة بغداد, العراق

الخلاصة

   يعتبر تحويل المساحات الخضراء والأراضي الزراعية إلى مناطق عمرانية من أهم آثار التحضر في المدن العراقية. حيث تعتبر المساحات الخضراء مطلبًا أساسيًا لأي مدينة لأنها تعزز أسلوب حياة صحي وتحافظ على المنظر الجمالي والبيئي للمناطق الحضرية. تهدف الدراسة الحالية إلى دراسة تأثير التحضر على الغطاء النباتي ودرجة حرارة سطح الأرض في محافظة بغداد، العراق. تم استخدام مؤشر الفروق العمراني المعياري

*Email: noor.younus1512m@coeng.uobaghdad.edu.iq

(NDBI)، ودليل الفروق الطبيعية للنباتات (NDVI)، ودليل الفروق القياسي للمياه (NDWI)، ودرجة حرارة
سطح الأرض (LST) لتحديد العلاقة بين المناطق الحضرية، ومناطق الغطاء النباتي، والمياه، ودرجة حرارة
الأرض لمدينة بغداد. تم استخدام بيانات المتجه لمدينة بغداد من الهيئة العامة للمساحة مع مخطط لاندسات
الموضوعي للأعوام 2004، 2008، وكذلك أداة التصوير التشغيلية لاندسات للأعوام 2013، 2017 ،
2021. لأجل فهم الارتباط بين المناطق الحضرية والمسطحات المائية، والمساحات الخضراء مع LST، تم
حساب معامل الارتباط بواسطة برنامج ArcGIS، وكذلك تم عمل مخطط لتقييم العلاقة بين العناصر. أظهرت
النتائج النهائية أن درجة حرارة سطح الارض زادت بمرور الوقت في مدينة بغداد بين عامي 2004 و 2021.
علاوة على ذلك، زادت المساحات المبنية من 17٪ في عام 2004 إلى 53.2٪ في عام 2021. في المقابل
وخلال نفس الفترة الزمنية، انخفضت نسبة المساحات الخضراء بشكل حاد بنسبة 39.7٪.

1. Introduction

Understanding environmental and human health effects depends on the relationship between a region's land use, land cover patterns, and the corresponding spatial and temporal temperature distribution [1]. Because of vegetation and water surface reduction brought on by urbanization, the earth's surface temperature rose due to anthropogenic heat emissions. Therefore, the increased land surface temperature is caused by increased artificial material coverage with high heat conductivities and capacities [2]. The severity of extreme climate events (heat waves, dust storms, drought, and desertification) and climate change are two of humanity's most significant environmental threats. Since rapid urbanization is nowadays an essential factor in global warming, the Urban Heat Island (UHI) impact undoubtedly impacts regional climate, environment, and socioeconomic development [3]. The hydrologic and vitality cycles are predicted to undergo significant changes as global surface temperatures keep rising due to the vulnerability of ecosystems to temperature increases brought on by climate change [4]. Green cover and exterior landscape are essential for walking, comfort, and relaxation and provide a diverse range of colors, shadings, linings, and natural shading from plants, which was preferred over artificial shading [5].

For scientists, environmentalists, planners, economists, policymakers, and anyone concerned about the sustainability of natural resources, it is crucial to identify changes in land use/cover (LULC) using remote sensing and Geographic Information Systems (GIS). One of the critical factors behind recent years' hotly contested global environmental change is LULC [6], where land use is the human inputs, utilization, and levels of management on the earth's surface, driven by the dynamic of consumption closely related to political, social, and economic actions, resulting in the modification of land cover. Land cover is the biophysical state of the earth's surface and upper subsurface [7]. Soil distribution and topography are uniquely impacted by the land cover change, leading to natural resource changes [8]. One of the factors causing LULC alterations is human activity [9]. Urbanization, or the conversion of non-agricultural land to urban, correlating to the population and economic expansion, caused a significant effect on macroclimate. Economic growth and population concentration have expanded densely populated areas on the outskirts of cities [10]. Urbanization areas have unplanted, impermeable surfaces with a large cover that reduces enormous amounts of solar energy. In addition, population growth, rising land prices within cities, the expansion of road systems, and people's reliance on automobiles caused people to move from urban centers to suburbs and rural areas, transforming broad agricultural into unplanned residential areas. As a result, on the outskirts, the percentage at which land turned from planted to unplanted was more than the percentage of inhabitants expansion; the cities and towns frequently spread in an unplanned manner on a metropolitan scale [4] and [11].

There is a growing literature that investigates urbanization's effect; for example, Kumari et al. (2018) [12] examined the NDBI, NDVI indices, and LST over Delhi, plus the Indian Survey toposheet (SOI). Landsat ETM+, TM, and OLI for 2003, 2010, and 2017, respectively, were adopted to calculate indicators such as NDBI, NDVI, and LST for 2003, 2010, and 2017. According to the study, the NDVI and land temperature have a negative correlation, whereas NDBI and land temperature have a positive correlation. All three temporal analysis algorithms of land surface temperature reveal an increase in Delhi's land surface temperature between 2003 and 2017. Hassoon and Ali 2021[13] studied the random urbanization growth in Baghdad during 2000-2015 and determined its impact on air temperature. It was found that Baghdad's surface temperature rose by 8 C° between 2000 and 2015. Surface temperature increases resulted in an increase in air temperature where the minimum temperature increased more than the maximum temperature (1.44 C ° and 0.76 C °, respectively). It was due to the growing expansion of urban areas as land use, particularly after 2003. The tracking of urban areas was achieved through supervised classification associated with the surface temperature records from Landsat TM and ETM+ satellite images.

The relationship between relative humidity and urbanization was investigated using data downloaded from the European Center for Medium-range Weather Forecasting (ECMWF) and remote sensing images for Baghdad [14]. They studied the consequences of land use/cover changes by monitoring how Baghdad's urbanization progressed quickly to understand the extent of its effects on the environment. Relative humidity (RH), temperature (T), and evaporation were used to support the process and analyze the Landsat 5 and Landsat 8 images for 2010 to 2020 using ArcGIS to confirm the changes seen in urban areas. The final results illustrated a direct correlation between rising urbanization and relative humidity levels and between the size of built-up areas and the rate at which local temperatures rise. Ali and Al-Ramahi 2020 [15] stated that there was a positive relationship between expanding urbanization and evapotranspiration rates by studying the urbanization expansion and vegetation decline using NDVI data in Baghdad during 2008-2018 from Landsat TM, and OLI for 2008, 2013, and 2018, in addition to evaporation rate data European Center for Medium-range Weather Forecasting (ECMWF) for the same period. The analysis process was done using two different methods; the first was supervised classification, while the second (NDI, NDVI) was used to obtain results that revealed that urban areas expanded by 4.4%, and water bodies fluctuated between decreasing in 2013 and increasing in 2018. Indicating that 2018 suffered from the highest evaporation rate and urbanization as well, referring to the positive correlation between them.

This study aims to use multitemporal satellite imagery and GIS techniques to generate Baghdad's LST and NDVI maps. In addition to assessing the relationship among LST and (NDVI, NDBI, and NDWI) to monitor the surface temperature with land cover change over the past 17 years, 2004-2021.

2. Study area and Datasets
Baghdad province (the capital of Iraq) was chosen as a study area between Latitude 32 48'00" N - 33 46'00" N and Longitude 43 51'00" E - 44 56'00" E. The total area of the study area is 5095.0 km^2 from 2018 to the present, while it was 5096.0 km^2 in 2004 and had expanded to 5196.0 km^2 from 2008 to 2017. The vector data from the General Authority of Surveying showed the area and shape differences with the neighboring provinces, especially in the East of Diyala and Wasit and a little bit in the South with Babil province. Baghdad has a semi-desert climate, hot and dry in summer, with some dust storms and rainy cold in winter.

The study area was subjected to many changes in land cover, land uses, average temperatures, and shape of the administrative borders from 2004 to 2021, Figure 1.
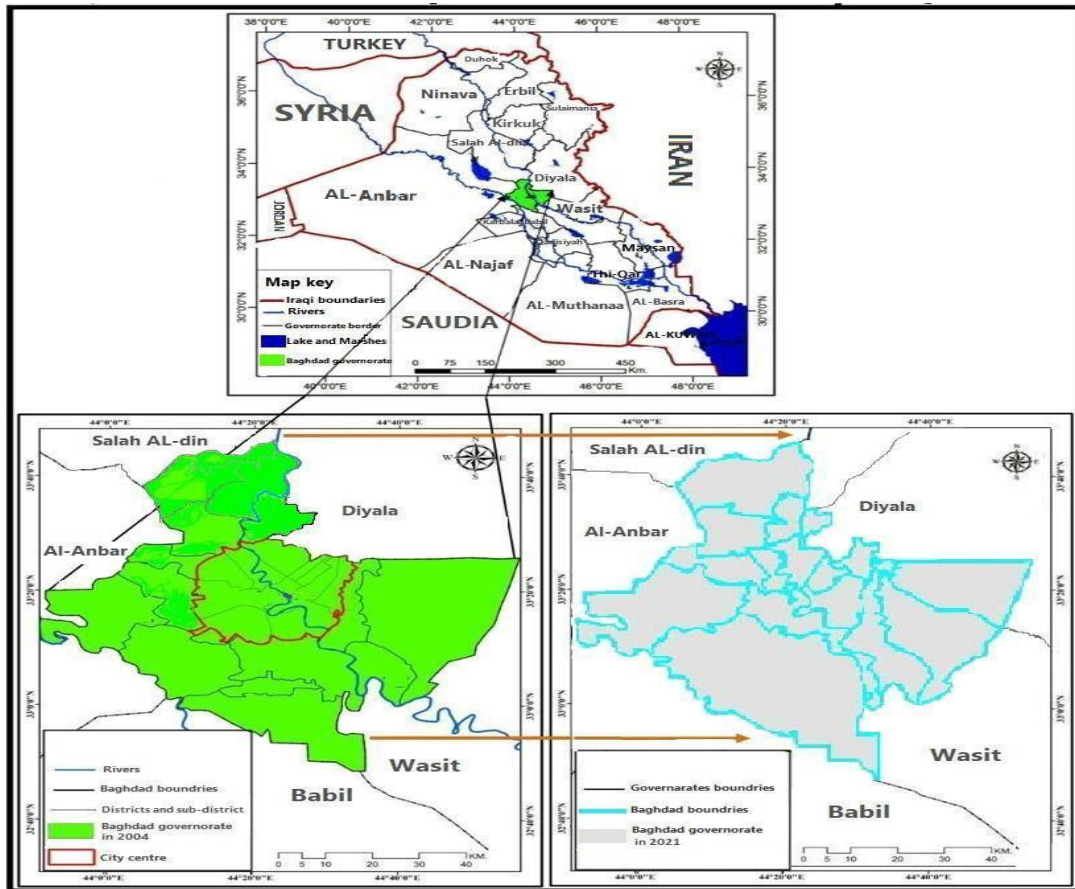
Figure1: The geographical location of the study area and the changes during the study period.

Satellite images were downloaded from the United States Geological Survey (USGS) Earth Explorer website. Landsat-TM satellites were downloaded for the period (July (2004 and 2008)), while (July (2013, 2017, and 2021)) were chosen from OLI/TIRS satellites with zero cloud coverage. The images were all level 2, a collection of two products that had been terrain corrected to level 1 (L1T). The L1T uses a Digital Elevation Model (DEM) for topographic accuracy and incorporates ground control points to provide systematic radiometric and geometric accuracy. All images were corrected for atmospheric, geometric, and radiometric effects [16]. All the images were downloaded in a (GeoTIFF) format with a resolution of 30×30 m on the World Geodetic datum System 1984 (UTM) projection, Zone 38 N path (168 and 169), and row 037.

3. Methodology

The main aim is to investigate the expansion of the built-up areas in Baghdad province during the study period 2004-2021 and find the correlation between NDVI, NDWI, and NDBI indices and LST. The following sections explain in detail the methods of land cover indices processing.

3.1. Normalized Difference Vegetation Index: According to equation 1 presented by [17], NDVI can be calculated using satellite images' red and near-infrared bands. These two bands were used in the calculation because NIR and red band electromagnetic spectrum absorption by chlorophyll is the highest. Plants absorb red and reflect only a tiny amount while reflecting a high amount of NIR [18].

$$NDVI = (NIR_{band} - Red_{band}) / (NIR_{band} + Red_{band}) \dots\dots\dots\dots\dots (1)$$

3.2. Normalized Difference Water Index: McFeeters 1996 [19] proposed the NDWI index to improve water-related landscape features. It is employed to identify and keep track of changes in the water bodies' content. Utilizing the green and near-infrared (NIR) spectral bands of satellite images. The following equation can calculate this index:

$$NDWI = (Green_{band} - NIR_{band}) / (Green_{band} + NIR_{band}) \dots\dots\dots\dots\dots (2)$$

3.3. Normalized Difference Built-up Index: This method was proposed by [20], based on using the Short-Wave Infrared (SWIR) and near-infrared bands (NIR). The following equation can calculate this index:

$$NDBI = (SWIR_{band} - NIR_{band}) / (SWIR_{band} + NIR_{band}) \dots\dots\dots\dots\dots\dots (3)$$

3.4. Land Surface Temperature (LST):

3.4.1. Landsat Thematic Mapper (TM)

Three techniques," the single channel method, split-window technique, and multi-angle method," were developed to derive surface temperature (Ts) from at-sensor satellite and auxiliary data [21].

Firstly, the image's digital number of thermal band 6 is transformed into spectral radiance using Eq. (4)

$$L\lambda = (Lmax\lambda - Lmin\lambda) / (Qcal\ max - Qcal\ min) \times (Qcal - Qcal\ min) + Lmin\lambda \dots\dots\dots\dots (4)$$

Where: L is the spectral radiation detected at Lmax, the satellite sensor's aperture. The radiation was measured by a satellite sensor and scaled to Qcalmax, Lmin. The satellite sensor picked up the radiation and scaled to Qcalmin, where Qcal is the maximum pixel value in DN that can be measured quantitatively. Lmax is the highest pixel value that can be accurately measured in DN. Qcalmin is the lowest pixel value that can be quantitatively measured in DN (given in the header file of the images).

Secondly, converting spectral radiance to satellite brightness temperature in kelvin (K), from which, under the assumption of uniform emissivity, one can derive the effective at-satellite temperature of the observed Earth-atmosphere system using Eq. (5).

$$T(K) = K2 / Ln [(K1 / L\lambda) + 1] \dots\dots\dots\dots\dots (5)$$

Where: (k) standardization calibration

T(k) is the efficient at-sensor brightness temperature, K1 = 667.76 (watts/(meter^2×ster×μm)) and K2 = 1260.56 (Kelvin) is standardization constants and given from metadata, and Lλ is the spectral radiance in watts /(meter^2×ster×μm).

Thirdly, the temperature was converted using Eq. (6) from Kelvin to Celsius in the final step.

$$T (°C) = T (K) - 273.15 \dots\dots\dots\dots\dots (6)$$

The previous process is illustrated in Figure 2, which shows the model builder of land surface temperature calculation. The model builder was performed using ArcGIS software, creating a new toolbox inside a new folder and then connecting the raster calculator with the model

through the parameters. Finally, the calculation was achieved automatically after giving an order of (Run); see Figure 2 for Landsat TM.
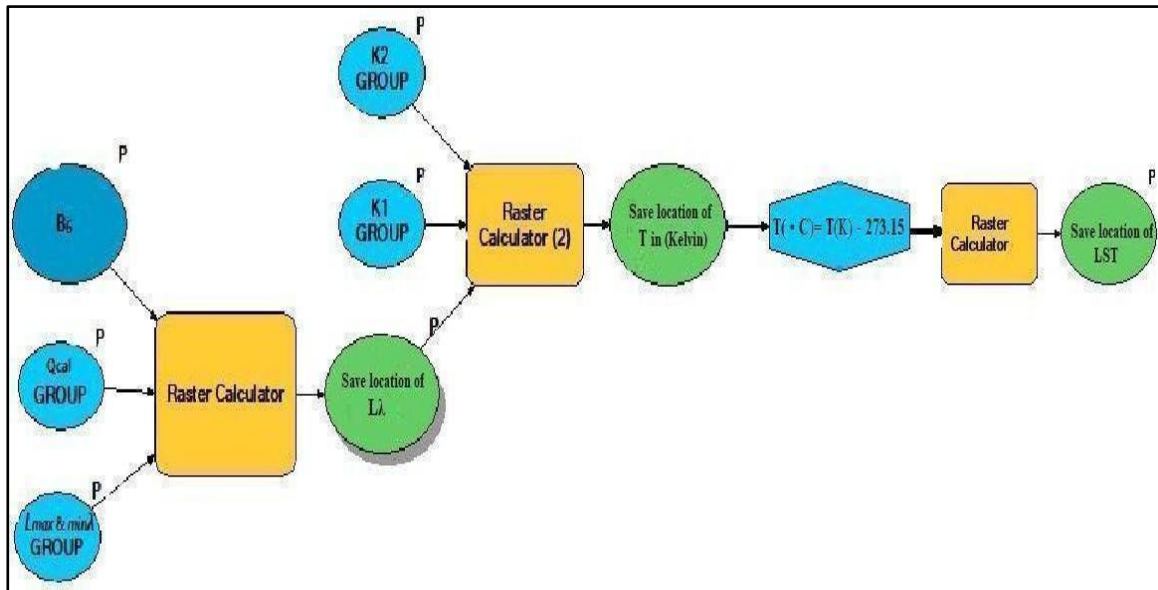

Figure 2: The model builder for Landsat TM.

3.4.2. Landsat operational land imager (OLI) and (TIRS) parameters:

The surface temperature recuperation from Landsat *(OLI/TIRS)* images, which was used to calculate LST, were described by the Landsat 8 handbook [22] as follows:

A. First, radiance rescaling factors from the metadata file were used to convert OLI and TIRS band data to radiance using Eq. (7).

$L\lambda = ML*Qcal + AL – Oi$ ……………… (7)

Where: $L\lambda$ is the spectral radiance of the top atmosphere's temperature (TOA), ML: a multiplicative rescaling factor derived from the metadata that is band-specific (RADIANCE MULTI-BAND), AL: The band-specific additive rescaling factor (RADIANCE ADD BAND) from the metadata, Qcal: standard product pixels that have been quantized and calibrated (DN), Oi: correction value (for Band#10 its = 0.29).

B. The second involved converting the spectral radiance TOA to the efficient at-satellite brightness temperature (BT) using the thermal steady provided in the image's MTL file using Eq. (8).

$BT = K2 / Ln [(K1/L\lambda) + 1]$ ……………… (8)

Where: $K1 = 774.885$ (watts/ (meter^2 × ster × μm)) and $K2 = 1321.0789$ (Kelvin) are calibration constants and given by metadata.

C. The normalized difference vegetation index (NDVI) was computed using the visible and near-infrared bands of Landsat (Eq. 1). Because the amount of vegetation present is a critical variable for LST estimation, the proportion of vegetation (Pv) was calculated by (Eq. 9) using the estimated NDVI [22].

$Pv = (NDVI − NDVIMIN) / (NDVIMAX − NDVIMIN)$ ……………… (9)

D. Land Surface Emissivity(ε) is crucial in estimating LST. ε can be calculated using Eq. (10)

$ε = 0.004 Pv + 0.986$ ……………… (10)

E. Malik et al. (2019) assert that Equation Eq. (11) can be used to translate satellite brightness temperature into land surface temperature (LST)

$LST = BT / \{1 + (λ*BT/C2)* Ln ε\}$ ……………… (11)

Where: LST the Land Surface Temperature in Celsius (ºC), BT brightness temperature, λ wavelength of emitted radiance (11.5 μm), C2 = 14,380 (constant), ε emissivity. $C_2 = (h*c/s)$,

where h: Planck's Constant=6.626*10^{-34}mk, s:Boltzmann constant =1.38*10^{-23}, c: Velocity of light = 2.998*10^8 m/sec.

The process of land surface temperature calculation was performed using a model builder, as shown in Figure 3
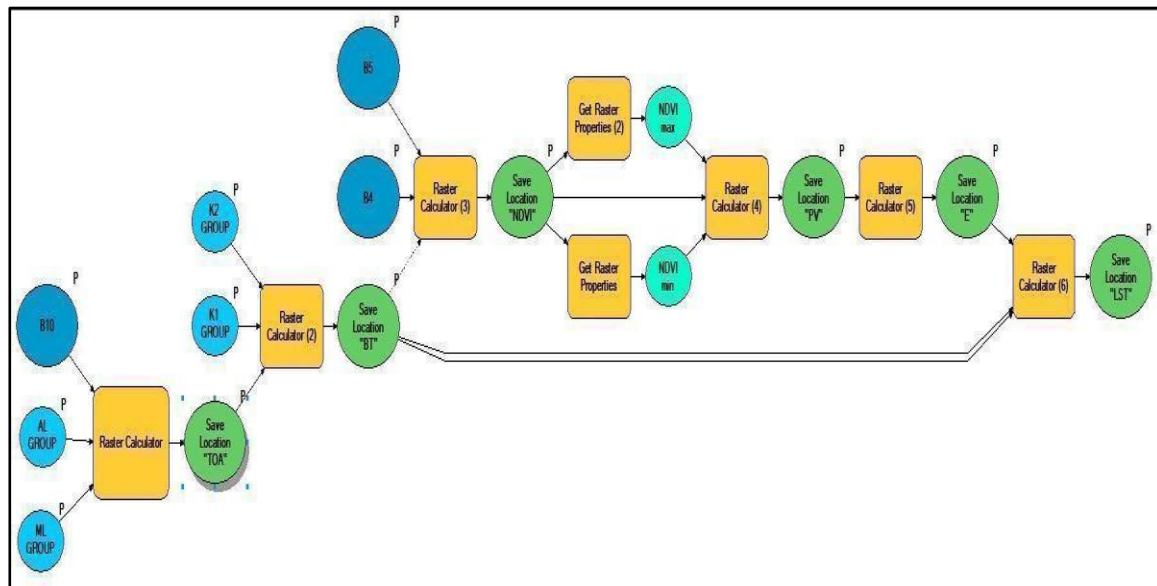
Figure 3: The model builder for calculating the land surface temperature.

4. Results and Discussion

The NDVI, NDWI, NDBI, and LST were calculated, and statistics graphs were generated to evaluate the relationship among indices. The LULC maps were compiled for 2004, 2008, 2013, 2017, and 2021. The final results illustrated that the built-up area has increased; urban areas have dramatically increased in size over the past 17 years, going from 865.5 km^2 to 2693.3 km^2 with an increase of 1827.8 km^2, Table 1.

Table 1: Demonstrates the green area, built-up area, water area, and open land over Baghdad.

Years	Green area (km^2)	Built-up (km^2)	Water area (km^2)	Open land (km^2)
2004	3390	865.5	60	780.5
2008	2488.6	1687	46	974.4
2013	2212.5	1854.5	73	1056
2017	1640.6	2610.6	74.4	870.4
2021	1354.8	2693.3	78.6	932.3

Urban sprawl covered 989 km^2 between 2004 and 2013 and decreased to 838.8 km^2 between 2013 and 2021. This suggests that after 2004, urban expansion increased intensively. Figure 4 presents urbanization rates in the Baghdad province between 2004 and 2021.
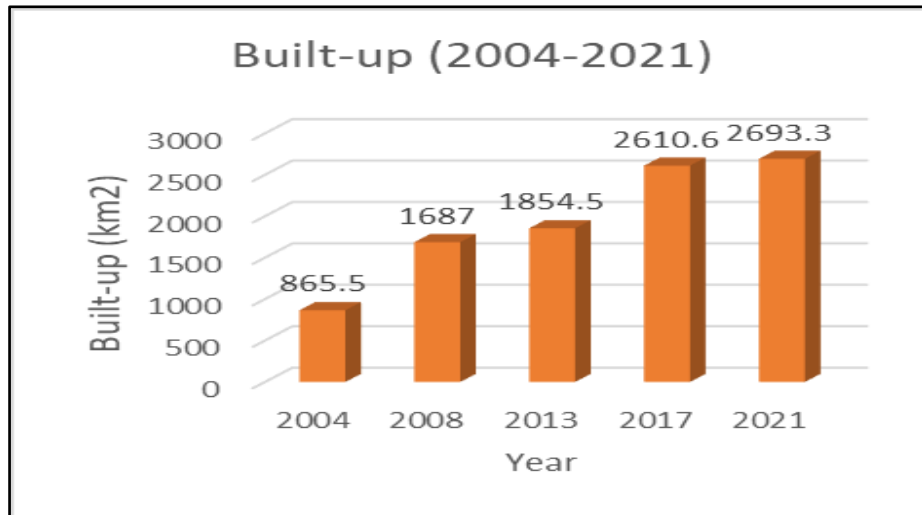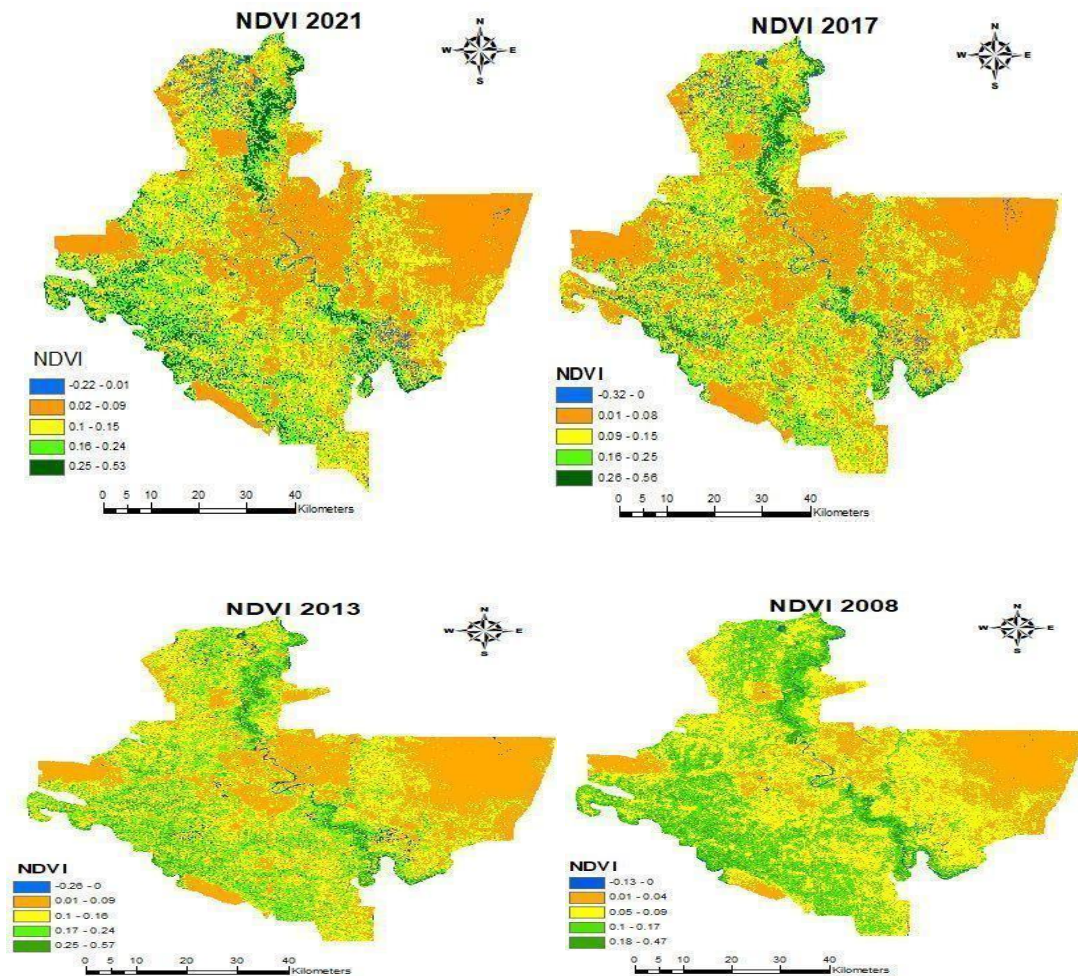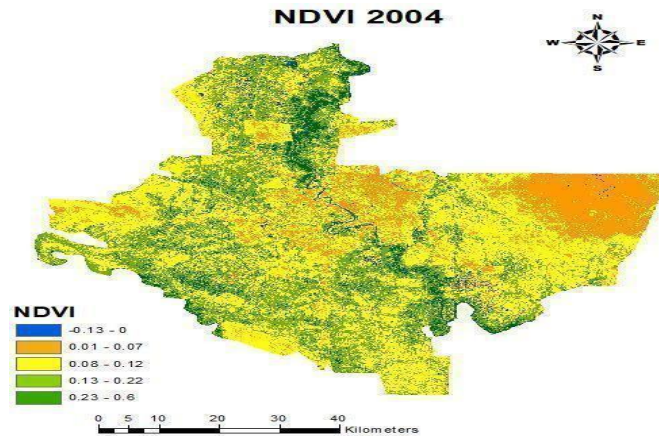
Figure 4: The built-up expansion during the research period.

The green area declined from 3390 km^2 to 1354.8 km^2, with a decrease of 2036 km^2 from 2004 to 2021. The green area climbs down 1177.5 km^2 from 2004 to 2013 and 857.7 km^2 between 2013 to 2021. The severity of the decrease in green areas was in the period between 2004 to 2013, Figures 5 and 6.

Figure 5: The deformation of the green area over Baghdad <u>province</u>.
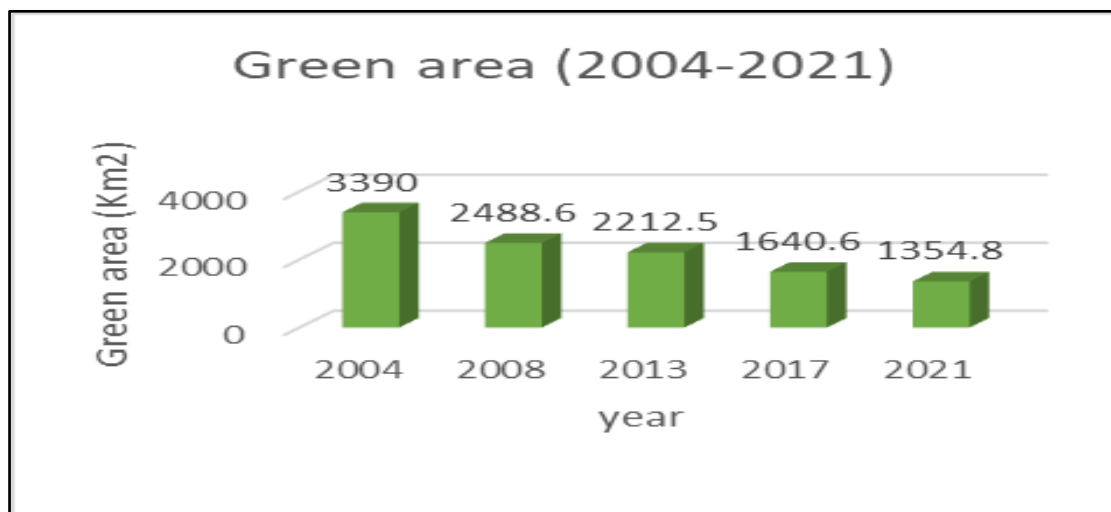
Figure 6: The declination of the green area during the research period.

The water area in Baghdad fluctuated from time to time depending on several factors, including the seasons, amount of rainfall, evaporation, and the amount of water released from the upstream countries. Figure 7 shows the results of the water area according to NDWI.
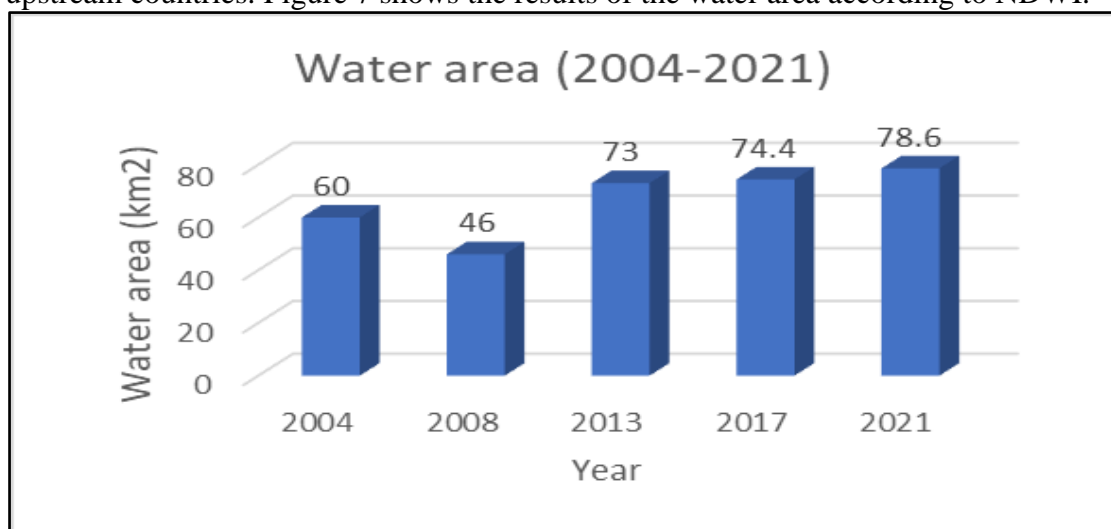
Figure 7: The fluctuation of the water area in Baghdad province.

The open land contains salty land, fertile and uncultivated soil, barren lands, and former military areas. This category increased noticeably after 2004.

The results of the surface temperature calculations indicated that the minimum surface temperature had risen about 1^0 C (from 46^0 C in 2004 to 47^0 C in 2021), while the maximum surface temperature had risen 2^0 C (from 58^0 C in 2004 to 60^0 C in 2021). Figure 8 clearly shows the land surface temperature distribution over Baghdad below.
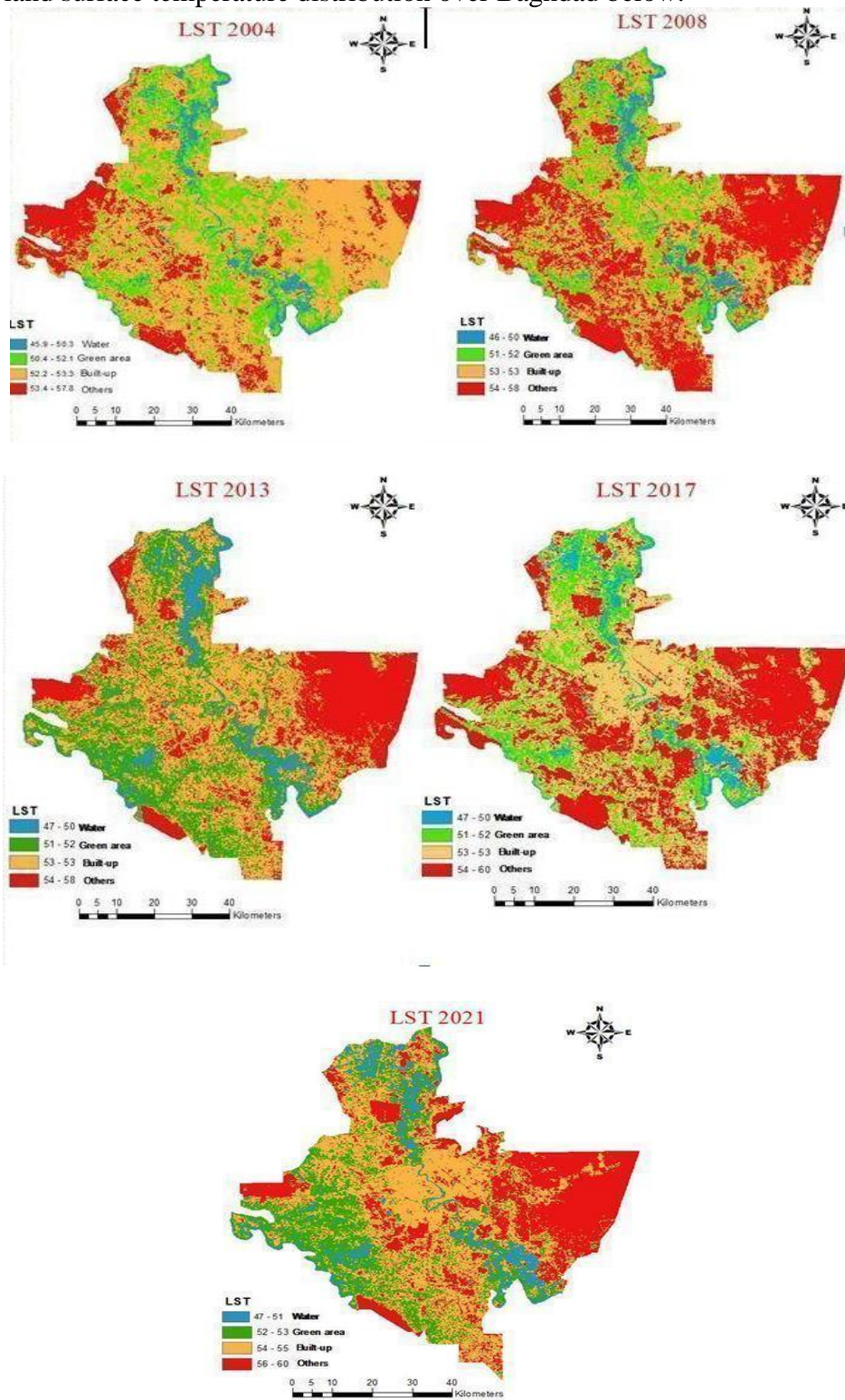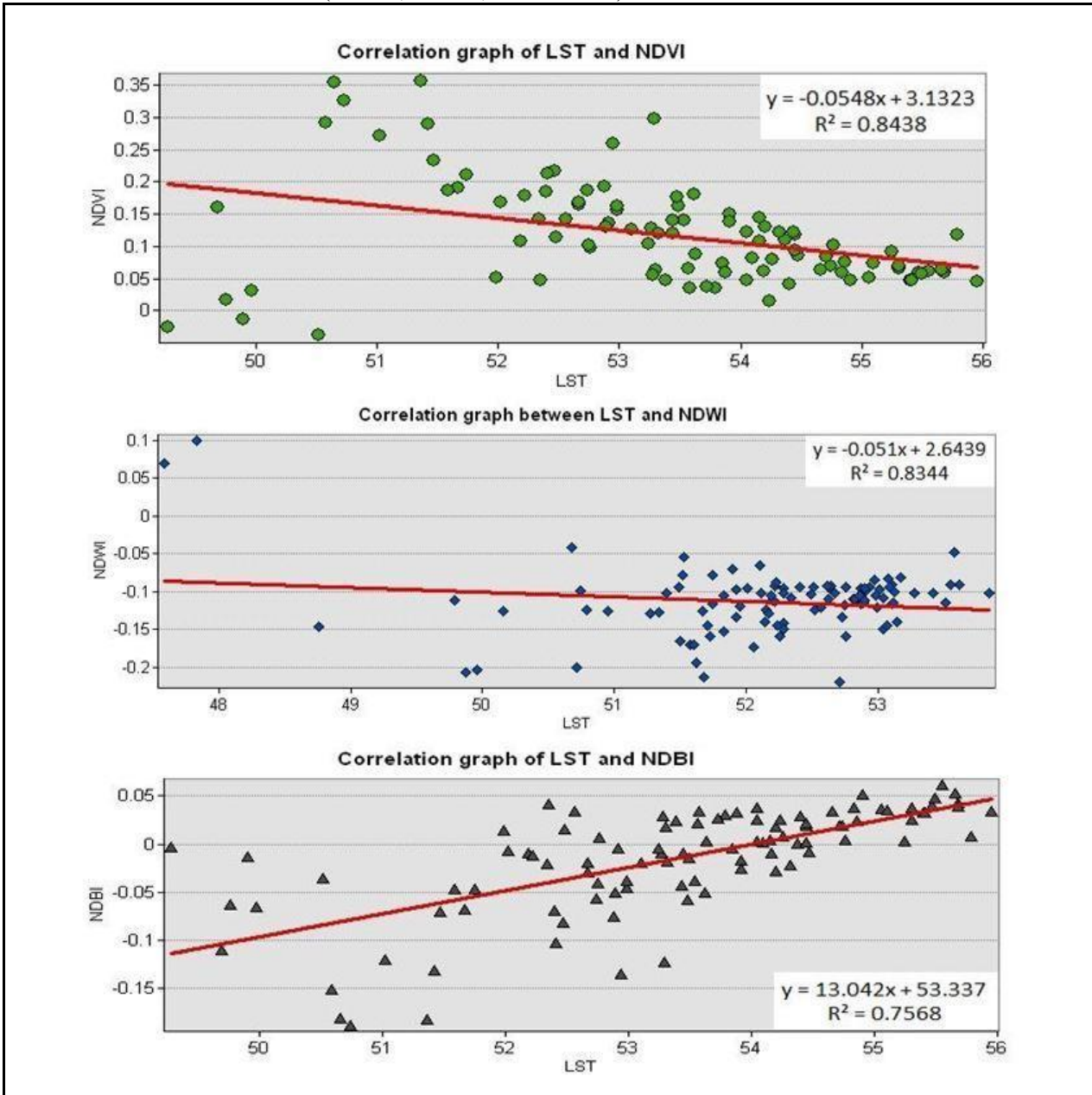

Figure 8: The land surface temperature distribution over Baghdad.

The final results showed that the water areas have the lowest LST while the open lands have the highest peak of LST. The LST in built-up areas varied between 52.2^0 C and 53.3^0 C in 2004, and it increased to 54^0 to 55^0 C in 2021, while the lowest peak was observed over the water area. The LST in open lands ranged from 53.4 to 57^0 C in 2004 and increased from 56^0 to 60^0 C in 2021. In contrast to the north-south geographic model, which has a low thermal gradient, the east-west geographic model has a high thermal gradient because more green area is towards the west and southwest of the city center than to the east. Figure 9 shows the relation between LST and (NDVI, NDBI, and NDWI).

Figure 9: The negative relationship between LST and (NDVI, NDWI), and the positive relationship between LST and NDBI.

The physical factors, such as topography, land use, and vegetation in city/urban areas, determine the land surface temperature of any location. The distribution of vegetative cover, human habitation, open space, bodies of water, and other features affects surface temperature [23]. A region with a high concentration of vegetation and water features is generally more

remarkable than a region with fewer greenery areas and water bodies because vegetation and water features regulate temperature. Figure 9 demonstrates the relationship between LST, NDVI, NDWI, and NDBI. The scatterplot shows an affirmative relationship between LST and NDBI, whereas the relationship between LST, NDVI, and NDWI was negative.

5. Conclusion

  The study demonstrates the rapid urbanization process's effects that result in changing land use patterns, causing constant changes in greenery distribution and constructed land. The clearing of vegetative cover for the building of residential complexes and commercial and industrial centers has resulted in the land surface temperature rises, which in turn affects the urban heat island (UHI). The study has effectively illustrated the deriving of LST, NDVI, and NDBI from the Landsat satellite images series to comprehend the environmental scenario in cities and identify the correlation between LST and built-up and vegetative cover over Baghdad. Thermal sensor data is essential for determining a land surface temperature from the Landsat satellite. All algorithms used for the temporal analysis of land surface temperature showed that Baghdad's land surface temperature increased between 2004 and 2021. The range of land surface temperatures increased from 45.9 to 57.8°C in 2004 to 47 to 60°C in 2021. The extracted data for LST, NDBI, NDWI, and NDVI are well-suited for understanding their correlation. It is visible that the average percentage of green area in Baghdad was 66.5 % in 2004 but drastically declined to 26.8 % at the district level in 2021. The LST and NDBI have a positive correlation; while a region with a high NDBI, in addition, to open land, exhibited a high LST, a district with a low NDVI exhibited a high LST and vice versa. Therefore, the current study demonstrated a significant correlation between a high density of built-up areas and a higher surface temperature, in addition to a high density of vegetation and a minimal surface temperature, demonstrates that the LST and NDWI have a negative correlation because vegetation and water bodies both have a cooling effect on the surface.

References

[1] S. Jr. and O. Rodgers, "Urban form and thermal efficiency: how the design of cities influences the urban heat island effect," *Journal of American Planning Association*, Nov. 2007, doi: 10.1080/01944360108976228. [Online]. Available: dx.doi.org/10.1080 /01944360108976228.

[2] S. Kumar, Dr. P. Udaya Bhaskar, and Dr. K. Padmakumari, "Estimation of Land Surface Temperature to Study Urban Heat Island Effect Using Landsat ETM+ Image," International *Journal of Engineering Science and Technology* (IJEST), Feb. 2012.

[3] A. Tekle, "Assessment of climate change impact on water availability of Bilate watershed, Ethiopian Rift Valley Basin," AFRICON, Nov. 2015, doi: 10.1109/AFRCON.2015.7332041.

[4] M. Zoran, R. Savastru, and D. Savastru, "Remote sensing image-based analysis for effects of urbanization on climate quantifying," Remote Sensing Image-Based Analysis for Effects of Urbanization on Climate Quantifying, 2013, doi: 10.1109/dese.2013.14 10.1109/dese.2013.14. [Online]. Available: 978-1-4799-5264-9/14© 2014 IEEE.

[5] J. Kamel, "IMPROVING OF GREEN COVER AND EXTERIOR LANDSCAPE DESIGN OF BAGHDAD UNIVERSITY' JADRIYAH CAMPUS'," *Iraqi J. Agric. Sci.*, vol. 48, no. 6 B, Nov. 2017.

[6] R. Hegazy and R. Kaloop, "Monitoring urban growth and land use change detection with GIS and remote sensing techniques in Daqahlia governorate Egypt," *International*

Journal of Sustainable Built Environment, Jun. 2015, doi: 2212-6090/Ó 2015 The Gulf Organisation for Research and Development. Production and hosting by Elsevier B.V. [Online]. Available: 10.1016/j.ijsbe.2015.02.005.

[7] E. Schulze, "Modelling Hydrological Responses to Land Use and Climate Change: A Southern African Perspective," *AMBIO,* vol. 29, Feb. 2000 [Online]. Available: www.jstor.org /stable /4314988.

[8] Q. Hu, D. Willson, and A. Akyuz, "Effects of climate and landcover change on stream discharge in the Ozark Highlands, USA," Environmental Modeling & Assessment volume, Mar. 2005, doi: 10.1007/s10666-004-4266-0. [Online]. Available: 10, pages 9–19 (2005).

[9] F. Lambin, J. Geist, and E. Lepers, "DYNAMICS OF LAND-USE AND LAND-COVER CHANGE IN TROPICAL REGIONS," *Annual Review Environment and Resources*, Jul. 2003, doi:10.1146/annurev.energy.28.050302.105459.

[10] V. Wilhelmi and H. Hayden, "Connecting people and place: a new framework for reducing urban vulnerability to extreme heat," *Environmental Research Letters*, Mar. 2010, doi: 10.1088/1748-9326/5/1/014021.

[11] A. K. Mohammed and F. K. M. Al Ramahi, "A study of the Effect of Urbanization on Annual Evaporation Rates in Baghdad City Using Remote Sensing," *Iraqi J. Sci.*, pp. 2142–2149, 2020.

[12] B. Kumari et al., "Satellite-Driven Land Surface Temperature (LST) Using Landsat 5, 7 (TM/ETM+ SLC) and Landsat 8 (OLI/TIRS) Data and Its Association with Built-Up and Green Cover Over Urban Delhi, India," *Remote Sensing in Earth Systems Sciences*, Nov. 2018, doi: doi.org/10.1007/s41976-018-0004-2.

[13] A. F. Hassoon and A.B. Ali, "Irregular urban Expansion and Its Effects on Air Temperature over Baghdad City using Remote Sensing Technique," *Iraqi Journal of Science*, pp. 2110–2121, Jul. 2021, doi: 10.24996/ijs.2021.62.6.36.

[14] S. M. Ahmed and F. K. M. Al-Ramahi, "Evaluate the Effect of Relative Humidity in the Atmosphere of Baghdad City urban expansion Using Remote Sensing Data," *eijs*, vol. 63, no. 4, pp. 1848–1859, Apr. 2022.

[15] A. K. M. Ali and F. K. M. Al Ramahi, "A study of the Effect of Urbanization on Annual Evaporation Rates in Baghdad City Using Remote Sensing", *eijs*, vol. 61, no. 8, pp. 2142–2149, Aug. 2020.

[16] "GIS Stake Exchange." [Online]. Available: https://gis.stackexchange.com/. [Accessed: Oct. 31, 2022]

[17] C. Gao, "NDWI—A normalized difference water index for remote sensing of vegetation liquid water from space.," *Remote Sensing of Environment*, vol. 58, no. 3, pp. 257–266, Dec. 1996, doi: doi.org/10.1016/S0034-4257(96)00067-3.

[18] D. Alessandro *et al.*, *Impact of Climate Change on Agricultural and Natural Ecosystems.* Firenze University Press, 2009, p. 244 [Online]. Available: library.oapen.org/handle/20.500. 12657 /54870.

[19] K. McFeeters, "The use of the Normalized Difference Water Index (NDWI) in the delineation of open water features.," *International Journal of Remote Sensing*, pp. 1425–1432, Apr. 2007, doi: 10.1080/01431169608948714.

[20] Zha, J. Gao, and S. Ni, "Use of normalized difference built-up index in automatically mapping urban areas from TM imagery," *International Journal of Remote Sensing*, vol. 24, no. 3, pp. 583–594, Nov. 2010, doi: doi.org/10.1080/01431160304987.

[21] M. Ullah, J. Li, and Bilal Wadood, "Analysis of urban expansion and its impacts on Land surface temperature and vegetation using RS and GIS, A case study in Xi'an City, China," Earth Systems and Environment, Jul. 2020, doi: doi.org/10.1007/s41748-020-00166-6.

[22] L. Mission, "Using the USGS Landsat 8 Product," *https://www.usgs.gov/landsat-missions/using-usgs-landsat-level-1-data-product*, 2016. [Online]. Available: landsat.usgs.gov. [Accessed: Oct. 29, 2022].

[23] Q. Weng, D. Lu, and J. Schubring, "Estimation of land surface temperature–vegetation abundance relationship for urban heat island studies," *Remote Sensing of Environment*, vol. 89, no. 4, pp. 467–483, Feb. 2004, doi: doi.org/10.1016/j.rse.2003.11.005.

[24] L. Chen, M. Zhao, X. Li, and Y. Yin, "Remote sensing image-based analysis of the relationship between urban heat island and land use/cover changes," *Remote Sensing of Environment*, vol. 104, no. 2,   pp.133–146, Sep. 2006, doi: 10.1016/j.rse.2005.11.016.